Norges miljø- og biovitenskapelige universitet

Masteroppgave 2023 30 stp
Faculty of Science and Technology

Comparing different techniques for stimulating neurons - a computational study

Birk Thorbjørnssønn Birkeland
Miljøfysikk og fornybar energi

Acknowledgements

I would first and foremost like to thank my supervisors, Geir Halnes and Marte Julie Sætra, for their valuable feedback and for their considerable time and effort in helping me write this thesis. I would also like to thank Gaute Einevoll for introducing me to the field of computational neuroscience, it has been my goal to write a masters thesis in this field since I first heard about it from him almost five years ago.

Abstract

When studying neurons we are often interested in measuring the response of the neuron to a certain stimulus. This stimulus is often in the form of an electric current entering the cell. However, there are different ways to force a current into a cell, and the way this is done may lead to different results even if the current strength is the same. Neurons may be stimulated for example with optogenetics or with the patch clamp technique, and stimulation currents can be made up of different mixes of ions. In computational models the stimulation is often modelled as simply an electrical current. That is, without considering the ions in the stimulation current and the subsequent change in ions concentrations. Many neuron models assume ion concentrations to be constant.

Using a neuron model that explicitly models ion concentrations over time allows us to study the effect of which ions are in the stimulation current. A model which includes both intracellular and extracellular space, as well as a way to introduce new ions from outside the system, allows us to study the effect of where the stimulation current is coming from.

We found differences in the response of the neuron to different ion stimulations, as well as differences between transmembrane and external injection current. In particular there was a strong effect of K^+, in that stimulation currents with more K^+ lead to higher firing rates. The differences between injection and transmembrane stimulation currents were small for currents with little or no K^+, but bigger differences were seen when the stimulation currents contained more K^+.

1 Introduction

When neurons are studied experimentally, experimenters often measure the response of the neuron to various types of electrical stimuli. Some examples of stimulation methods are electrode stimulation and optogenetic stimuation. Computational models also often include methods of stimulation. These may be modelled simply as an electrical current, with the assumption that only the strength of the current is relevant to the response of the neuron. However, the currents used for stimulation are composed of various ions. Because there are many different mixes of ions that can be used in stimulation current, the mix of ions, as well as the strength of the current, may have some effect on the response of the neuron. Many common neuron models, such as the Hodgkin-Huxley model, focus on the net current while assuming the concentrations of ions to be constant[1] [2]. Another example is the Pinzsky-Rinzel model [3]. This may be a good approximation in most cases, however concentrations can not be completely constant.

There have also been made models that explicitly keep track of ions, keeping a consistent relationship between ion concentrations, charge, currents, potentials, and so on. An example of this is the electrodiffusive Pinsky-Rinzel (edPR) model from Sætra et al. [4]. This is a four-compartment expanded version of the

Pinsky-Rinzel model from [3]. The Pinsky-Rinzel model is a two-compartment model of a hippocampal CA3 neuron[3]. In the edPR model, stimulation of the neuron is done by forcing a current of K^+ ions over the membrane from an extracellular to an intracellular compartment.

It is a reasonable question whether the ions in the stimulation current, and the resulting changes in concentrations, affect the response. Another question is whether it makes a difference where the stimulation current is coming from. There exist different methods to stimulate a neuron, and different ways to implement stimulation in a computational model. These are the questions that this thesis will address, using the edPR model from Sætra et al. [4] .

In this thesis, two methods of stimulating neurons are considered. One of these is modelled as a flow of ions entering the soma from outside the model system. This is meant to represent a patch clamp technique where a glass pipette is put onto the side of the cell, and current is injected[2] [5]. This can be considered an electrode. Current goes into the cell from the pipette, which is typically filled with a solution that is similar to the intracellular solution of the cell [5]. The pipette can also be filled with other solutions, such as NaCl[6].

The other method studied in this thesis is a transmembrane current, a flow of ions across the membrane from an extracellular compartment that is inside the system. In this case the stimulation current is internal to the system, no new ions are forced into the system. The same model is used as for the external injection current, so ions can move into and out of the system at this boundary, although there will not be a net current at this boundary.

This thesis has three main goals:

1. The original edPR model is a closed system, and a stimulation current in this system is modelled as a current over the membrane from the extracellular to the intracellular space. To allow a more realistic modelling of external stimuli, the model will be expanded to describe an open system where stimulation by an external pipette can be included.

2. To study whether it makes a difference whether the stimulation is modelled as an external current or as a cross-membrane current, given that the current and the ions carrying it are the same.

3. To study whether the mix of ions in the stimulation current affects the response of the neuron, or if only the current strength matters.

2 Background

2.1 Biological background

Neurons are capable of generating electrical signals called action potentials. An action potential is seen as a rapid increase in the membrane potential, called depolarization, followed by a decrease in the potential back to the initial resting level, which is called repolarizaton[2]. A neuron can be modelled as an electrical circuit, with familiar electrical components such as current sources and

capacitors[2]. However, the electrical currents in a neuron are not electrons moving in a copper wire. The currents in neurons are made up of ions. There are several types of ions involved in charging and discharging the neuron membrane. Both positively and negatively charged ions are involved in the electrical activity of the cell. These ions move through the cell membrane of the neuron in response to various stimuli, and in doing so polarize and depolarize the cell membrane[2].

The potential difference across the membrane at any time is caused by there being different charge densities on either side of the membrane. This means the concentrations of the various ions must be different on the inside and the outside of the cell. The solutions of the intracellular space (ICS) and the extracellular space (ECS) are different, with the ECS typically having more sodium and the ICS having more potassium[2].

2.2 Computational background

There are many types of computational models of neurons, and models can be made to explore different aspects of a neuron [2]. A model is always a simplification of the thing it is meant to represent. Even a single neuron is a highly complex system, with many processes going on simultaneously. Fortunately, we do not need to model every single process in a cell to learn something useful from the simulations. Many models in computational neuroscience are based directly on electrical potentials and currents, and do not explicitly model ion dynamics. These models may include membrane potentials, ion specific reversal potentials and conductances, as well as gating variables and more. The model can be based on an equivalent circuit, without explicitly modelling the spatial dimensions of the cell. This type of model can accurately reproduce action potentials [2].

Slightly more complex models may include ion concentrations and the spatial dimensions of the cell [2] [4]. This is the type of model that is used in this study. This type of models allows us to explore the effects of various stimuli on the ion concentrations, and the effects of ion concentrations on the behavior of the cell.

The main goal of this thesis is comparing different methods of stimulating neurons using the electrodiffusive Pinsky-Rinzel (edPR) model described in Sætra 2020 [4]. The original edPR model is an ion-conserving model which explicitly models ion concentrations for Na^+, K^+, Cl^-, and Ca^{2+}, as well as immobile ions labelled as X^-. Two stimulation methods will be compared; transmembrane and electrode.

The edPR model has four compartments, two intracellular and two extracellular. Each compartment has a fixed volume, and between each touching compartment there is a fixed area. At all times the concentrations of each ion in each compartment are tracked. Ions can flow between the compartments both across and along the membrane. The movement of the ions produce currents because the ions are charged. That is, fluxes of ions are calculated between the compartments, and currents can be calculated from the number of ions crossing a boundary per second. Intracellular fluxes flow between the two in-

tracellular compartments, the soma and the dendrite. Extracellular fluxes flow between the two extracellular compartments, representing the spaces outside of the soma and outside of the dendrite. Membrane fluxes flow between the extracellular and intracellular compartments, both in the soma and in the dendrite, with some differences between the compartments. Potentials are also calculated from the charge of the ions in the compartments.

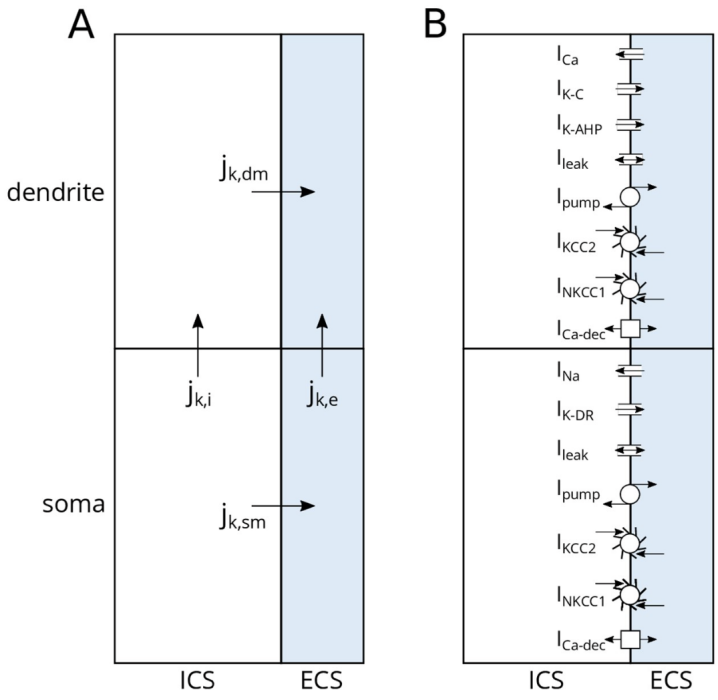

Figure 1: *The architecture of the four compartment edPR model from sætra 2020 [4], showing ion channels on the neuron model membrane. This figure is taken from Sætra et al. [4].*

The model contains ion channels which allow ions to move across the membrane. All of the membrane mechanisms in the five compartment model are the same as in the original edPR model with four compartments from [4]. The ion channels are shown in the figure 1, and short descriptions of them are shown in table 1.

The ion channels are described with the Hodgkin-Huxley-formalism. In general, the ion channels are described by an equation on the form of

$$I_k = \bar{g}_k \cdot m^a \cdot h^b \cdot (\phi - E_k) \tag{1}$$

where $\bar{g}_k$ is the maximum conductance for ion k, and ϕ is the membrane potential. The gating variable m is the probability of a gating particle to being

Table 1: *Membrane ion channels of the edPR model.*

Flux designation	Short description
$j_{k,\text{leak}}$	Leak
j_{Na}	Sodium
j_{K-DR}	Delayed rectifier potassium
j_{Ca}	Voltage-dependent calcium
j_{K-C}	Calcium dependent potassium
j_{K-AHP}	Voltage dependent potassium afterhyperpolarization
j_{Ca-dec}	Intracellular Ca^{2+} decay
j_{pump}	$3Na^+/2K^+$ pump
j_{nkcc1}	$Na^+/K^+/2Cl^-$ cotransporters
j_{kcc2}	K^+/Cl^- cotransporters

in the open state, a is the number of gating particles in each gate. The gating variable h is the probability of a gating particle to being in the open state, b is the number of gating particles in each gate. The reversal potential, E_k, of ion k is calculated using the Nernst equation:

$$E_k = \frac{RT}{z_k F} \ln\left(\frac{[k]_e}{\gamma_k [k]_i}\right) \tag{2}$$

where R is the gas constant, T is the temperature, γ is the fraction of ion type k that are free to move in the cell, and $[k]_i$ and $[k]_e$ are the intracellular and extracellular concentrations of ion k, respectively[4].

The intracellular and extracellular flux densities are given by the Nernst-Planck equation:

$$j_{k,\text{i}} = -\frac{D_k}{\lambda_i^2} \frac{\gamma_k([k]_{di} - [k]_{si})}{\Delta x} - \frac{D_k z_k F}{RT\lambda_i^2} [\bar{k}]_i \frac{\phi_{di} - \phi_{si}}{\Delta x} \tag{3}$$

$$j_{k,\text{e}} = -\frac{D_k}{\lambda_e^2} \frac{([k]_{de} - [k]_{se})}{\Delta x} - \frac{D_k z_k F}{RT\lambda_e^2} [\bar{k}]_e \frac{\phi_{de} - \phi_{se}}{\Delta x} \tag{4}$$

where ϕ_{si} and ϕ_{di} are the electrical potentials of the soma and dendrite intracellular compartments, respectively. Likewise, ϕ_{se} and ϕ_{de} are the electrical potentials of the soma and dendrite extracellular compartments, respectively. z_k is the ion number of ion type k, D_k is the diffusion constant of ion k, F is Faraday´s constant, λ_e and λ_e are the tortuositities of the intracellular and extracellular spaces, respectively[2].

3 Methods

In order to model the stimulation of the neuron with an electrode some changes must be made to the edPR model. In the original model the system of four compartments is closed. No ions go into or out of the system, and the total

charge is preserved. To model the electrode stimulation, ions need to be put into the system. This means ions must also have a way to leave the system in order to keep the total charge preservation. To achieve this a fifth compartment is added. This is called the external ghost compartment, and is connected to the dendrite extracellular compartment. In the external compartment all ion concentrations are assumed to be constant, so a movement of charge into this compartment is effectively removed from the system. The five-compartment modification to the edPR model necessitates a new set of equations for the time derivatives of the ion concentrations as well as for the potentials between the compartments. The membrane currents as well as the cellular mechanisms are the same as in the original model.

3.1 Expanded version of the edPR model

The expanded neuron model has five compartments; the soma intracellular (si), the soma extracellular (se), the dendrite intracellular (di), the dendrite extracellular (de), and the external ghost compartment (ex). This is slightly different from the four-compartment electrodiffusive Pinsky-Rinzel model in Sætra 2020 (edPR model) [4] which this model is based on, because the external ghost compartment is added. This was done so that it would be possible to introduce a current into the system from outside the system. In the original edPR model the four compartments make up a closed system, where the total number of each ion type is always conserved in the system. In the original model ions can only move between the four compartments, but no ions can enter or leave the system. Because of this, a stimulation current in the original edPR model must be modelled exclusively as a movement of charge between compartments. The external ghost compartment is added so that ions can move to and from this compartment, so that the charge anti-symmetry of the system is conserved when additional ions are introduced to another part of the system. Without this compartment any flux of ions into the system would accumulate, and the total charge of the system would change.

In the external ghost compartment all ion concentrations are constant. Thus, any ion that moves into this compartment is effectively removed from the system. Because the concentrations in this compartment are constant at the level they were at the start of the simulation, diffusion to and from this compartment will work to return concentrations in the system to the initial conditions when no stimulation current is applied.

The addition of the ghost compartment leads to some changes in the dynamics of the system. Importantly, the electric potential in this compartment is defined to be equal to zero. This is in contrast to the original edPR model where the potential is defined to be zero in the dendrite extracellular compartment[4]. Other equations must be updated to account for this change.

The other major change to the edPR model is the addition of a stimulation current coming from outside the system. This is for modelling stimulation of the neuron by electrode. Changes must be made to the equations so that the charge anti-symmetry is maintained when this current is active, which includes

charge conservation in the system. This means that the same amount of current going into the system from the stimulation current must be going out of the system to the external ghost compartment. Note that the numbers of each ion in the system are not conserved, only charge. For example, if a potassium ions enters the soma through the stimulation current and a sodium ion leaves the dendrite extracellular compartment, charge is conserved.The architecture of the expanded model is shown in figure 2.

The model is implemented in Python. It is solved with the $solve_ivp$ function from scipy.integrate, using the LSODA method. All constants and initial values are the same as used in Sætra et al. [4].

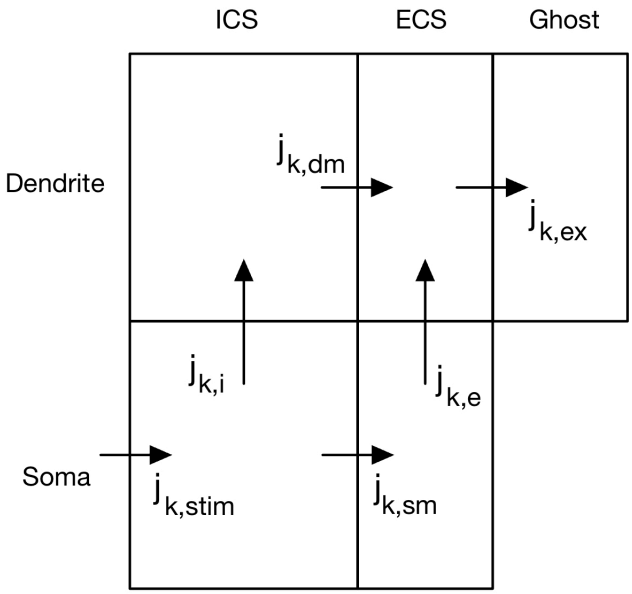

Figure 2: *The architecture of the expanded edPR model with five compartments. The ghost compartment and the ion flux, $j_{k,ex}$, is added, as well as the stimulation $j_{k,stim}$ from outside the system. All of the membrane fluxes making up $j_{k,sm}$ and $j_{k,dm}$ are the same as in the original edPR model from [4] as seen in figure 1 B.*

3.2 Currents and fluxes

The ion fluxes across the membranes are the same as in the edPR model, they are not changed for the expanded model. Some other fluxes must be defined or redefined. The flux into the ghost compartment must be defined, as well as a way to convert the desired stimulation current into a flux of ions into the soma.

The flux density into the external ghost compartment is given by the Nernst-

Planck equation:

$$j_{k,ex} = -\frac{D_k}{\lambda_e^2}\frac{[k]_{ex} - [k]_{de}}{\Delta x} - \frac{D_k z_k F}{RT\lambda_e^2}\bar{[k]}_{ex}\frac{\phi_{ex} - \phi_{de}}{\Delta x} \tag{5}$$

where ϕ_{de} is the electrical potentials of the dendrite extracellular compartment. The potential of the external ghost compartment, ϕ_{ex}, is defined to be equal to zero.

The intracellular currents are then:

$$i_i = -\frac{F}{\lambda_i^2 \Delta x}\sum_k D_k z_k \gamma_k([k]_{di} - [k]_{si}) - \frac{F^2}{RT\lambda_i^2\Delta x}\sum_k D_k z_k^2 \bar{[k]}_i(\phi_{di} - \phi_{si}) \tag{6}$$

$$i_e = -\frac{F}{\lambda_e^2 \Delta x}\sum_k D_k z_k([k]_{de} - [k]_{se}) - \frac{F^2}{RT\lambda_e^2\Delta x}\sum_k D_k z_k^2 \bar{[k]}_e(\phi_{de} - \phi_{se}) \tag{7}$$

where γ_k is the proportion of ion k which is free in the cell, D_k is diffusion constant of ion k, and Δx is the distance between compartments. λ_i and λ_e are the tortuosities of the intracellular and extracellular space. $\bar{[k]}_i$ and $\bar{[k]}_e$ are the average concentrations in the intracellular and extracellular compartments, respectively. That is,

$$\bar{[k]}_i = \frac{1}{2}([k]_{si} + [k]_{di}) \tag{8}$$

$$\bar{[k]}_e = \frac{1}{2}([k]_{se} + [k]_{de}) \tag{9}$$

The current out of the system is:

$$i_{ex} = -\frac{F}{\lambda_e^2 \Delta x}\sum_k D_k z_k \gamma_k([k]_{ex} - [k]_{de}) - \frac{F^2}{RT\lambda_e^2\Delta x}\sum_k D_k z_k^2 \bar{[k]}_{ex}(\phi_{ex-\phi_{de}}) \tag{10}$$

where $[k]_{ex}$ is the average concentration between the dendrite extracellular compartment and the external ghost compartment:

$$\bar{[k]}_{ex} = \frac{1}{2}([k]_{ex} + [k]_{de}) \tag{11}$$

The currents in the Nernst-Planck equations can be separated into diffusion currents and field currents:

$$i_{diff,i} = -\frac{F}{\lambda_i^2 \Delta x}\sum_k D_k z_k \gamma_k([k]_{di} - [k]_{si}) \tag{12}$$

$$i_{diff,e} = -\frac{F}{\lambda_e^2 \Delta x}\sum_k D_k z_k([k]_{de} - [k]_{se}) \tag{13}$$

$$i_{diff,ex} = -\frac{F}{\lambda_e^2 \Delta x} \sum_k D_k z_k ([k]_{ex} - [k]_{de}) \tag{14}$$

$$i_{field,i} = -\sigma_i \frac{\phi_{di} - \phi_{si}}{\Delta x} \tag{15}$$

$$i_{field,e} = -\sigma_e \frac{\phi_{de} - \phi_{se}}{\Delta x} \tag{16}$$

$$i_{field,ex} = -\sigma_{ex} \frac{\phi_{ex} - \phi_{de}}{\Delta x} \tag{17}$$

where the conductivities are defined as:

$$\sigma_i = \frac{F^2}{RT\lambda_i^2} \sum_k D_k z_k^2 [\bar{k}]_i \tag{18}$$

$$\sigma_e = \frac{F^2}{RT\lambda_e^2} \sum_k D_k z_k^2 [\bar{k}]_e \tag{19}$$

$$\sigma_{ex} = \frac{F^2}{RT\lambda_e^2} \sum_k D_k z_k^2 [\bar{k}]_{ex} \tag{20}$$

3.3 Ion conservation

To keep track of ion concentrations we solve four differential equations for each ion species k. The concentrations in the external ghost compartment are defined to be constant:

$$\frac{d[k]_{si}}{dt} = -j_{k,sm} \cdot \frac{A_s}{V_{si}} - j_{k,i} \cdot \frac{A_i}{V_{si}} + I_{stim} \cdot \frac{f_k}{V_{si} \cdot F} \tag{21}$$

$$\frac{d[k]_{di}}{dt} = -j_{k,dm} \cdot \frac{A_s}{V_{di}} + j_{k,i} \cdot \frac{A_i}{V_{di}} \tag{22}$$

$$\frac{d[k]_{se}}{dt} = +j_{k,sm} \cdot \frac{A_s}{V_{se}} - j_{k,i} \cdot \frac{A_e}{V_{se}} \tag{23}$$

$$\frac{d[k]_{de}}{dt} = +j_{k,dm} \cdot \frac{A_d}{V_{si}} + j_{k,e} \cdot \frac{A_e}{V_{de}} - j_{k,ex} \cdot \frac{A_{ex}}{V_{de}} \tag{24}$$

$$\frac{d[k]_{ex}}{dt} = 0 \tag{25}$$

where z_k is the ion number of ion k, F is the Faraday constant. V refers to volume and [k] to concentrations, where the subscripts si and di refer to the soma intracellular and dendrite intracellular compartments, respectively, while the subscripts si and di refer to the soma intracellular and dendrite intracellular compartments, respectively. The subscript ex refers to the external ghost

compartment. A_i is the area between the soma intracellular and dendrite intracellular compartments. A_e is the area between the soma extracellular and dendrite extracellular compartments. A_ex is the area between the dendrite extracellular compartment and the external ghost compartment. A_s and A_d are the areas between the intracellular and extracellular compartments, for the soma and dendrite, respectively.

The fluxes, j, are shown in figure 2. $j_{k,sm}$ and $j_{k,dm}$ are the fluxes of ion k crossing the dendrite and soma membranes, respectively. $j_{k,i}$ and $j_{k,e}$ are the intracellular and extracellular fluxes. $j_{k,ex}$ is the flux of ion k from the dendrite extracellular compartment to the external ghost compartment. I_{stim} is the stimulation current that enters the soma. Finally, f_k is the fraction of the stimulation current which is carried by ion k. An expression for f_k will be defined later.

3.4 Deriving expressions for the potentials ϕ

An expression must be defined for the potentials in each of the five compartments. The major changes from the edPR model is the redefinition of which compartment has the constant zero potential, and how the addition of the injection current affects the potentials. The latter is important because the potential differences are what drives many of the fluxes in the system, including the fluxes into and out of the ghost compartment. That is, the potentials need to ensure that the ions of the stimulation current do not simply accumulate, so that the system in total remains electroneutral.

A reference point for the potentials may be defined arbitrarily. In the external ghost compartment concentrations are already defined to be constant, and now the potential ϕ_{ex} in this compartment is defined to be 0:

$$\phi_{ex} = 0 \tag{26}$$

Another constraint is that the membrane is assumed to be a parallel plate capacitor. The membrane always separates a charge Q on one side from an opposite charge Q on the other side:

$$\phi_m = \frac{Q}{C_m} \tag{27}$$

where C_m is the capacitance of the membrane and Q is the charge on the membrane. Using the membrane capacitance per unit area c_m instead the expression becomes:

$$\phi_m = \frac{Q}{C_m} = \frac{Q}{c_m A_m} \tag{28}$$

where A_m is the area of the membrane.

Bulk electroneutrality is also assumed. The net charge associated with the ion concentrations in a given compartment must be identical to the membrane

charge in this compartment:

$$\phi_{di} - \phi_{de} = \frac{F \sum_k z_k [k]_{di} V_{di}}{c_{dm} A_{dm}} \tag{29}$$

$$\phi_{si} - \phi_{se} = \frac{F \sum_k z_k [k]_{si} V_{si}}{c_{sm} A_{sm}} \tag{30}$$

where z_k is the ion number of ion k, F is the Faraday constant, $[k]_{di}$ and $[k]_{si}$ are the concentrations of ion k in dendrite and soma intracellular compartments, respectively, V_{di} and V_{si} are the volumes of the dendrite and soma intracellular compartments, respectively, c_{dm} and c_{sm} are the membrane capacitances per unit area of the dendrite and soma, respectively, and A_{dm} and A_{sm} are the areas of the dendrite and soma membranes, respectively.

A further constraint is charge anti-symmetry between the two sides of the capacitive membrane:

$$Q_i = -Q_e \tag{31}$$

To ensure charge anti-symmetry at all times we need to make sure the initial charges are anti-symmetrical, and that the currents uphold the anti-symmetry. The membrane currents always maintain charge anti-symmetry, because a charge going through the membrane has to appear on the other side of the same membrane. However, we need to make sure that the axial currents also uphold the charge anti-symmetry. This leads to two expressions, one for the soma and one for the dendrite, respectively:

$$A_i i_i = -A_e i_e - I_{stim} \tag{32}$$

$$A_i i_i = -A_e i_e + A_{ex} i_{ex} \tag{33}$$

Combining these two equations gives

$$I_{stim} = A_{ex} i_{ex} \tag{34}$$

which is equivalent to the statement that the current going out of the system is the same as the current going into the system. This means that the total charge in the system is conserved.

Equation 32 can be used to find an expression for ϕ_{se}. Substituting in expressions for i_{drift} from 15 and 16 gives

$$-A_i i_{diff,i} + A_i \sigma_i \frac{\phi_{di} - \phi_{si}}{\Delta x} = -A_e i_{diff,e} + A_e \sigma_e \frac{\phi_{de} - \phi_{se}}{\Delta x} + I_{stim} \tag{35}$$

Using equation 30 and solving 35 for ϕ_{se} gives the following expression for ϕ_{se}:

$$\phi_{se} = (\frac{\Delta x}{A_e \sigma_e + A_i \sigma_i})(I_{diff} + \frac{A_e \sigma_e}{\Delta x} \phi_{de} + \frac{A_i \sigma_i}{\Delta_x} \phi_{di} - \frac{A_i \sigma_i}{\Delta x} \frac{F \sum k z_k [k]_{si} V_{si}}{c_m A_s} - I_{stim}) \tag{36}$$

where I_{diff} is defined as

$$I_{diff} = -A_e i_{diff,e} - A_i i_{diff,i} \tag{37}$$

It follows from equation 34 that the total charge in the system is conserved. This means that the stimulus current going into the soma must be equal to the current going out of the system into the external ghost compartment.

Expressing 34 using the ion flux gives

$$I_{stim} = FA_{ex} \sum_k j_{k,ex} z_k \tag{38}$$

where $j_{k,x}$ is defined by equation 5. Combined, this gives

$$\sum_k z_k (-\frac{D_k}{\lambda_e} \frac{[k]_{ex} - [k]_{de}}{\Delta x} - \frac{D_k z_k F}{RT\lambda_e^2} \frac{1}{2} ([k]_{ex} + [k]_{de}) \frac{\phi_{ex} - \phi_{de}}{\Delta x}) = \frac{I_{stim}}{FA_{ex}} \tag{39}$$

Solving this equation gives the following expression for ϕ_{de}

$$\phi_{de} = \frac{\frac{\Delta x \lambda_e^2 I_{stim}}{FA_{ex}} - \sum_k z_k D_k ([k]_{de} - [k]_{ex})}{\frac{F}{2RT} \sum_k z_k^2 D_k ([k]_{de} + [k]_{ex})} \tag{40}$$

3.5 Stimulation protocols

To study the effect of different stimuli we tested: i) 2 different current strengths, ii) 2 stimulation methods, transmembrane and external injection, and iii) 8 different ions mixes in the stimulation current. This gives $2 \cdot 2 \cdot 8$ different stimulation protocols, so that in total, 32 protocols are tested. Eight ion mixes are defined, and each ion mix is used for both injection and cross membrane current. Each ion mix and type of current is also tested for both high and low current. In all protocols the stimulation current is into the soma, although it would also be possible to put this current into the dendrite.

For the injection currents, the different ions mixes represent the solution in the pipette that injects the current. These are listed in table 2. In protocol A the solution in the pipette has similar concentrations as the in the intracellular space (ICS) of the cell. In protocol B the solution in the pipette has similar concentrations as the extracellular space (ECS) outside the cell. Protocol C represents a pipette filled with sodium chloride solution, and protocol D represents a potassium chloride solution. Protocol E is modelled as a movement of only sodium ions. Protocol F is a flow of only potassium ions. Protocol G is likewise a flow of only chloride ions.

Protocol H models a current of ions that are immobile in the cell, labelled as X^- in the model. Because these ions are immobile they can not move between compartments like the other ions do, and they will accumulate in the soma.

For all protocols the current going into the cell is positive. This means that positive ions will move into the cell, and negative ions will move out, according to the ions mix in the stimulation current.

Table 2: *Protocols for testing*

Protocol	Type of solution	Ions in stimulus current
A	ICS	K^+, Na^+, Cl^-
B	ECS	K^+, Na^+, Cl^-
C	NaCl	Na^+, Cl^-
D	KCl	K^+, Cl^-
E	Na	Na^+
F	K	K^+
G	Cl	Cl^-
H	Immobile ions	X^-

For each stimulation protocol the input to the model is simply the electrical current that will be put into the soma compartment as well as the type of solution in the current. In the edPR model all currents are modelled explicitly as changes in the concentrations of ions. This must also be the case for the stimulation current. Thus, for each protocol there must be an expression relating the current we want to put into the cell to a change in the concentrations of ions. This expression will depend on the diffusion constants as well as the concentrations of the ions in the stimulus current. The change in the concentration of ion species k associated with a stimulation current I_{stim} is given by:

$$\frac{d[k]_{si}}{dt} = f_k \frac{I_{stim}}{F z_k V_{si}} \tag{41}$$

where F is Faraday´s constant, z_k is the ion number of ion species k, V_{si} is the volume of the intracellular soma compartment, and $[k]_{si}$ is the concentration of ion species k in the intracellular soma compartment. Here, f_k is the fraction of the total current I_{stim} which is carried by the ion k. For the protocols where the stimulation current consists of only on ion species, f is equal to 1.

For the protocols with more than one ion species in the stimulation current the diffusion constants and relative concentrations must be taken into consideration.

The fraction f_k is given by the flux of ion k divided by the total flux of ions for a given I_{stim}. This fraction is found by considering the current for each ion type k given by the Nernst-Planck equation:

$$J_k = J_{k,diff} + J_{k,drift} = -D_k\left(\frac{d[k]}{dx} + \frac{z_k F}{RT}[k]\frac{d\phi}{dx}\right) \tag{42}$$

[2] where $J_{k,diff}$ and $J_{k,drift}$ are the diffusion and drift contributions to the total flux, D_k is the diffusion constant of ion k, [k] is the concentration of k, ϕ is potential, and x is distance. F, R, and T are still the Faraday constant, universal gas constant, and temperature, respectively.

The diffusion current contribution to the stimulation current is assumed to be negligible. Thus, the flux of ion k given a potential difference $\frac{d\phi}{dx}$ is

$$J_k = J_{k,drift} = -\frac{D_k F}{RT} z_k[k] \frac{d\phi}{dx} \tag{43}$$

where D_k is the diffusion constant of ion k, F is Faraday´s constant, R is the universal gas constant, T is the temperature, $[k]$ is the concentration of ion k, and z_k is the ion number of ion k.

However, f_k is the fraction of change in concentration of ion k compared to the total change in concentration for all ions. Because of this, fluxes in both directions must be counted as the same. A negative ion moving out of the soma will contribute equally to the current as a positive ion moving into the soma. Thus, the absolute value of z_k must be used in the calculation of f. The direction of the movement of ion k is decided by equation 41.

The combined flux will simply be the sum of the fluxes, for each ion, k. This gives the fraction f as:

$$f = \frac{\frac{D_k F}{RT}|z_k|[k]\frac{d\phi}{dx}}{\sum_k \frac{D_k F}{RT}|z_k|[k]\frac{d\phi}{dx}} = \frac{\frac{F}{RT}\frac{d\phi}{dx} D_k|z_k|[k]}{\frac{F}{RT}\frac{d\phi}{dx}\sum_k D_k|z_k|[k]} \tag{44}$$

The flux of calcium ions in the stimulation current is assumed to be negligible, because the concentration and diffusion constant of calcium ions are relatively low[4]. This means that the total stimulation flux J is a sum of J_k over sodium, potassium, and chloride.

For the stimulation current, diffusion currents are

$$f_k = \frac{J_k}{J} = \frac{D_k|z_k|[k]}{D_{Na}[Na^+] + D_K[K^+] + D_{Cl}[Cl^-]} \tag{45}$$

where $[Na^+]$, $[K^+]$, and $[Cl^-]$ are the proportions of sodium, potassium, and chloride ions in the stimulation current, respectively. For example, in protocol C, $[Na^+]$ is 1, $[Cl^-]$ is 1, and $[K^+]$ is 0. The calculated values for f_k are shown in table 3.

Table 3: *Calcuated values of* f_k

Protocol	Type of solution	f_{Na}	f_K	f_{Cl}	f_X
A	ICS	0.103	0.836	0.0612	0
B	ECS	0.0181	0.399	0.583	0
C	NaCl	0.396	0	0.604	0
D	KCl	0	0.491	0.509	0
E	Na	1	0	0	0
F	K	0	1	0	0
G	Cl	0	0	1	0
H	Immobile ions	0	0	0	1

3.6 Low current - sustained firing

To test the neurons response to a low stimulation current sustained over a longer period of biological time, a 90 second simulation is run for each protocol. In these protocols, the neuron is stimulated with a current of 40 pA starting at 5 seconds and ending at 85 seconds. A 40 pA current was chosen because this gives a reasonable firing rate to compare protocols, and gives the model time to reach a stable firing rate in the given time.

3.7 High current - depolarization block

A depolarization block can happen when the neuron is stimulated with a very high current. If the current is high enough, the membrane potential does not return to the baseline between each action potential. The lowest membrane potential between action potentials will get progressively higher over time, until the neuron is no longer able to fire action potentials. While the strong current is still applied, the neuron will not fire.

This is studied in this thesis by finding a current which is sufficient to lead to a depolarization block for all protocols, and then applying this current for all protocols and comparing the amount of time before depolarization block begins. The depolarization block is defined to begin at the time of the last action potential fired with a maximum potential of above 0 V.

3.8 Which comparisons are interesting?

The model allows us to compare between stimulation current injected from an external source and a stimulation current crossing the soma membrane from inside the system. The model also allows us to compare between the different ions mixes that make up the stimulation current. In each case the change in concentrations in the soma associated with a current I_{stim} is given by equation 41 with f given by equation 45.

For the protocols with a low current, the model responds with firing action potentials, and over time the firing rate of the model will stabilize. The firing rate that the model stabilizes at is one thing to compare between the protocols. Firing rates can be compared between external injection and transmembrane stimulation currents for any given ion mix, or between different ion mixes with the same stimulation method. As the model stabilizes the ion concentrations will also reach new dynamic equilibriums, and these can be compared between the models. The ion concentrations may be informative in studying why the different protocols result in different responses.

For the protocols with a high current, the model responds by first firing action potentials very rapidly, before reaching a depolarization block. The time before the model reaches depolarization block can be compared, to look for differences between stimulation methods and stimulation current ion mixes.

4 Results

4.1 Membrane potentials and firing rates

Simulations with a relatively low stimulation current were run to study the model during sustained action potential firing. These simulations allow for study of firing rates for different protocols. For all 16 protocols a simulation was run for 90 seconds of biological time, with a stimulation current of 40 pA starting at 10 seconds and ending at 85 seconds. The firing rate produced by this current varies between the protocols, but in general is close to 1 Hz.

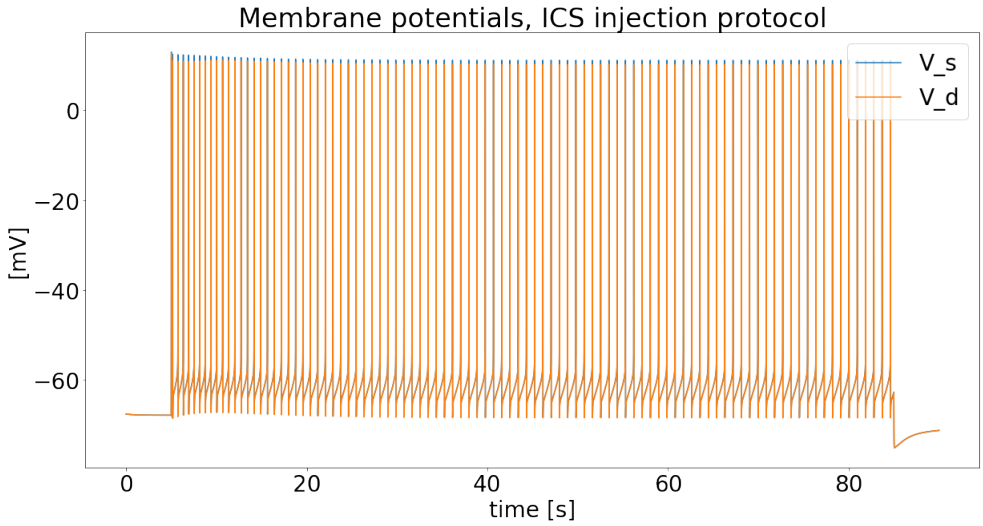

Figure 3: *Membrane potentials during the ICS protocol with injection of current into soma from external source.*

Figure 3 shows the membrane potentials during the 90 second simulation with 40 pA ICS ion mix stimulation current. It is visible in the figure how the neuron fires a bit more rapidly in the beginning and then reaches a stable firing rate. This can be compared to figure 4 which shows the membrane potentials during the 40 pA ECS ion mix stimulation current. In this case the firing rate is lower, seen by the wider spacing between the spikes in the membrane potentials. Still, the same pattern is visible of the neuron firing more rapidly to begin with before reaching a stable firing rate. For a comparison to a transmembrane stimulation protocol, and example is shown in figure 9. Compared to the ICS injection protocol in figure 3, this shows the same shape with a lower firing rate, although the firing rate is still higher than for the ECS injection protocol in figure 4.

Table 4 summarizes the number of spikes fired during one simulation for each protocol. The average number of spikes for the soma injection protocols is slightly higher than the average number of spikes for the soma cross-membrane

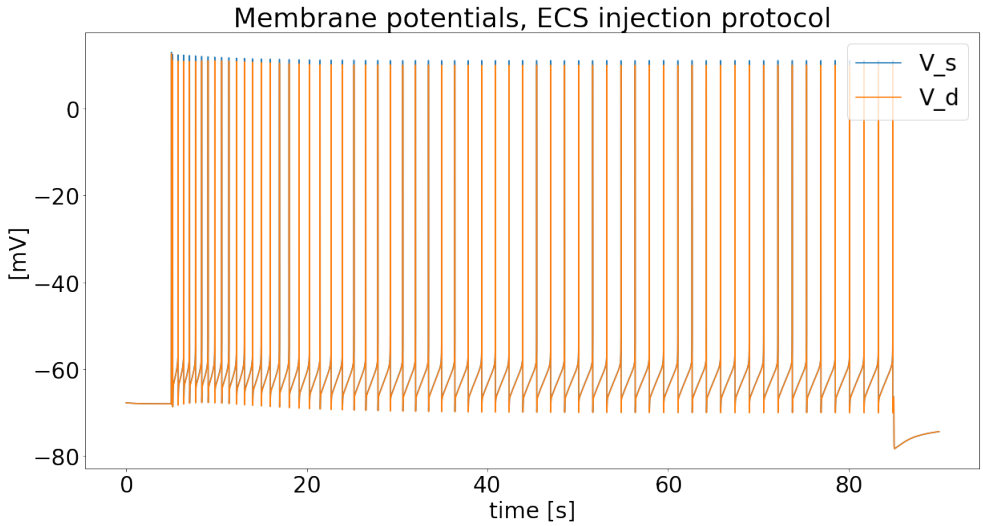

Figure 4: *Membrane potentials during the ECS protocol with injection of current into soma from external source.*

protocols. However, the standard deviation is also higher for the injection protocols.

It might be more interesting to compare the differences in firing rate between stimulation with injection current and with cross-membrane current, for the same ions mixes. The ECS ion mix gives the same number of action potentials in both cases. The NaCl, Na, and Cl protocols all result in only one more action potential fired in the cross-membrane protocols than in the injection protocols. The differences in firing rate between injection and transmembrane stimulation are smaller for these four ion mixes than for the remaining ones. These four ion mixes are also made up entirely or mostly of sodium and/or chloride, with relatively low potassium. So, the protocols with the smallest differences between injection and transmembrane stimulation were the ones where the stimulation current was made up entirely or mostly of sodium and/or chloride.

The previously mentioned protocols stand in contrast to the protocols with ion mixes that consist entirely or mostly of potassium. These are the ICS, KCl, and K protocols. For all of these protocols the neuron fires more action potentials when stimulated with injection current than when stimulated with cross-membrane current. For the K protocols the difference is 13, between 102 for the injection and 89 for the cross-membrane protocols. The ICS protocols give 10 more action potentials fired for the injection current than for the cross-membrane, and the KCl protocols give 6 more. This is interesting, as the difference seems to increase with increasing potassium content in the stimulation current.

The figures 5 and 6 show the time between spikes over time for all injection

Protocol ion mix	Soma injection	Soma cross-membrane
ICS	95	85
ECS	63	63
$NaCl$	62	63
KCl	82	76
Na	58	59
K	102	89
Cl	63	64
X	135	259
$Average, excl.X$	75	71.3
$Std.dev., exclX$	17.9	12.0

Table 4: *Total number of action potentials fired by the neuron during each protocol. Stimulation current is 40 pA for all protocols. The bottom two entries are the average and the standard deviation, respectively, of the number of spikes in each stimulation method. The stimulation protocols with the immobile ions, X, are not included in the average and standard deviation.*

and cross-membrane stimulation protocols, respectively. One effect is especially clear when looking at figure 5 for the injection current protocols, and that is that the graphs seem to group together in two groups. Again, the stimulation protocols with more potassium stand out from the ones with more sodium and chloride.

The stimulation protocols with more potassium lead to a higher firing rate than the ones with more sodium and/or chloride. This effect is apparent in both the injection and cross-membrane protocols, but especially in the injection protocols.

The two protocols where the stimulation current consists of the immobile ions, the X ions, do not lead to stable firing rates. As these ions are immobile in the cell, they will simply accumulate and never move out of the compartment they are in either by diffusion or by electrical drift. This means that in order to maintain charge anti-symmetry, other ions must move around to make up for the added negative charges in the soma interior, and in the case of the cross membrane X-current also for the subtracted negative charges in the soma exterior compartment. The more immobile ions that are added, the more the concentrations of the other ions will be distorted from the initial conditions. Unlike for the other protocols, the concentrations will not be able to return to the initial equilibrium.

4.2 Ion concentrations during low current stimulation

Ion concentrations vary with each action potential. This effect is similar for all protocols, as the mechanisms of the action potentials are the same. However, a long simulation where the model reaches a stable firing rate makes it possible to study effects of the different protocols on timescales longer than the

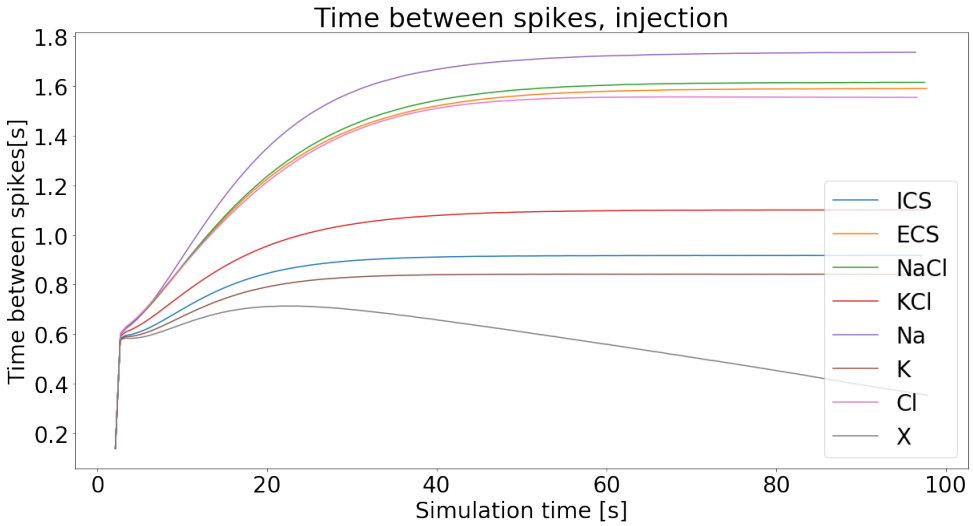

Figure 5: *Time between spikes over time for the different stimulation protocols, with the same stimulation current for all protocols. Injection of current into soma from external source*

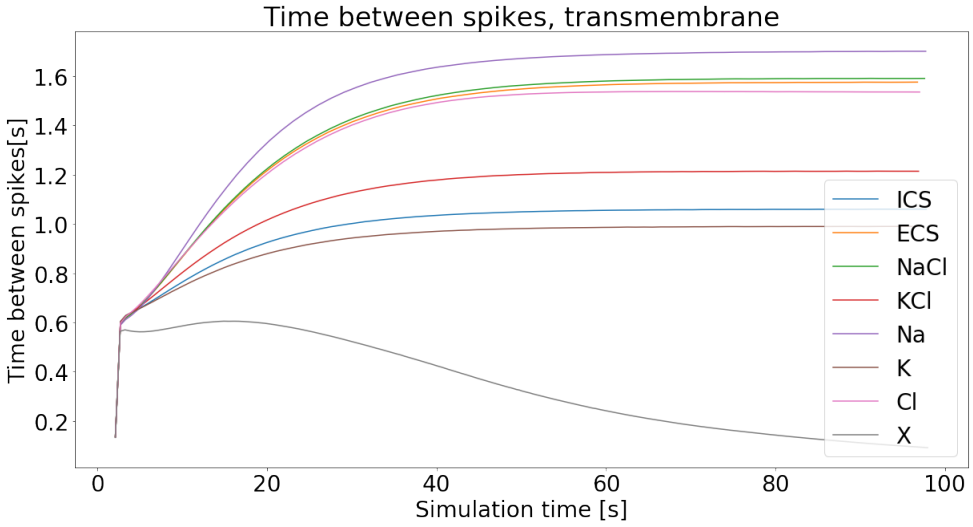

Figure 6: *Time between spikes over time for the different stimulation protocols, with the same stimulation current for all protocols. Current into soma across the membrane from soma external compartment.*

AP frequency. The concentrations of each ion in each compartment may be plotted over time. Figure 7 shows the changes in concentrations of all mobile

ions during the 90 second simulation with the 40 pA injection current with ICS ion mix. Note that the concentrations of all ions in the external ghost compartments are constant by definition. Also note that the concentrations of the immobile ions, X, are constant in all compartments, and are not plotted. All of the concentrations vary with each action potential, which is what makes the concentration plots jagged. However, the concentrations also show trends on longer timescales during the stimulation time, where the concentrations reach new dynamic steady state equilibriums as the firing rate of the neuron stabilizes. The concentrations continue to oscillate around the new equilibriums with each action potentials.

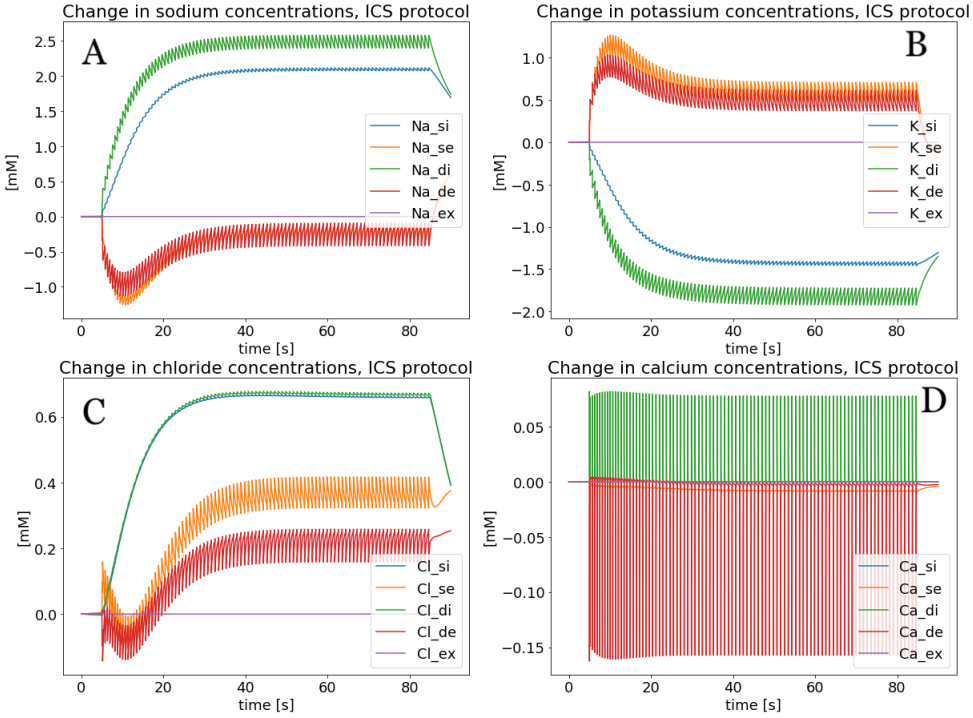

Figure 7: *Changes in concentration of ions during the ICS protocol with injection of current into soma from external source. Subplots A, B, C and D show changes in* Na^+, K^+, Cl^-, *and* Ca^{2+}, *respectively.*

Figure 8 shows the equivalent with the ECS ion mix. Again, the concentrations oscillate with each action potential while also showing trends over time. Note that the shapes of the graphs here are different than in figure 7, for example in the plots of chloride concentrations. In the ICS protocol the di and si chloride concentrations reach a new equilibrium which is higher than the initial concentrations. In contrast, in the ECS protocol these same concentrations reach equilibriums that are below the initial concentrations. This is expected,

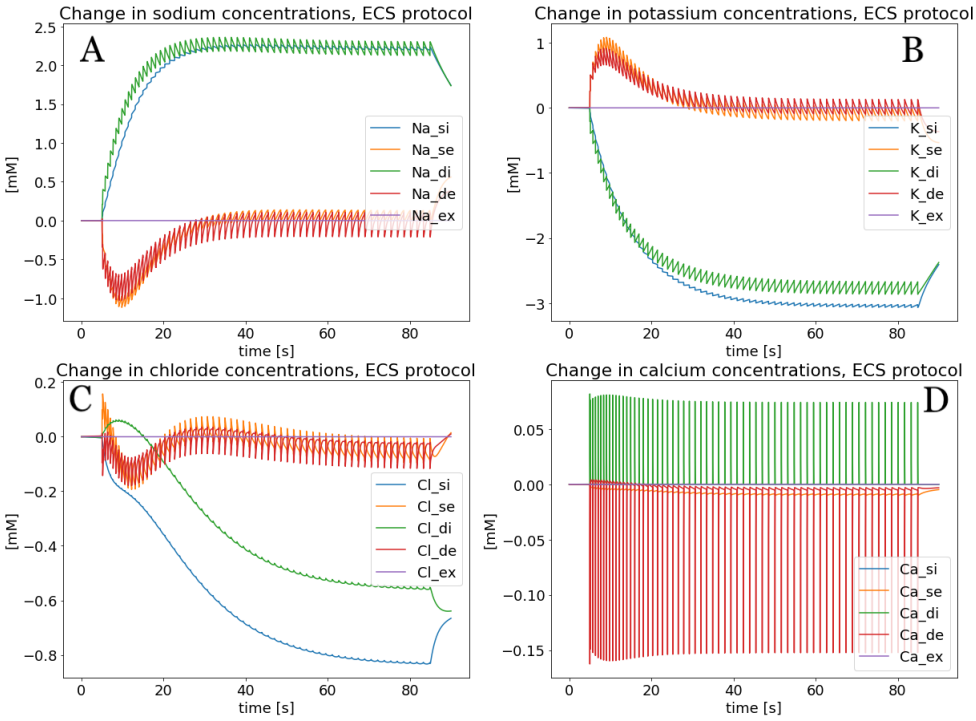

Figure 8: *Changes in concentration of ions during the ECS protocol with injection of current into soma from external source. Subplots A, B, C and D show changes in* Na^+*,* K^+*,* Cl^-*, and* Ca^{2+}*, respectively.*

as the ECS current moves more Cl^- out of the cell.

Figure 7 of concentrations plots for the ICS injection stimulation current can also be compared to figure 10 shows the same plots for the ICS cross-membrane stimulation current. There are visible differences in the plots of extracellular K^+, which might be significant given the relatively low concentrations of K^+ in the extracellular space. The differences in Na^+ are proportionally smaller.

From the previous subsection about firing rates it can be concluded that K^+ in the injection current has an important effect. The protocols mentioned as examples in this subsection are the ICS cross-membrane, the ICS injection, and the ECS injection, of which ICS injection has the highest firing rate. The concentration plots in figures 7 B, 8 B, and 10 B, show that the ICS injection protocol leads to the biggest change in extracellular K^+. As the extracellular K^+ concentrations are quite small at around 4.3 mM[4], these changes are proportionally quite large. This is discussed further in section 4.4.

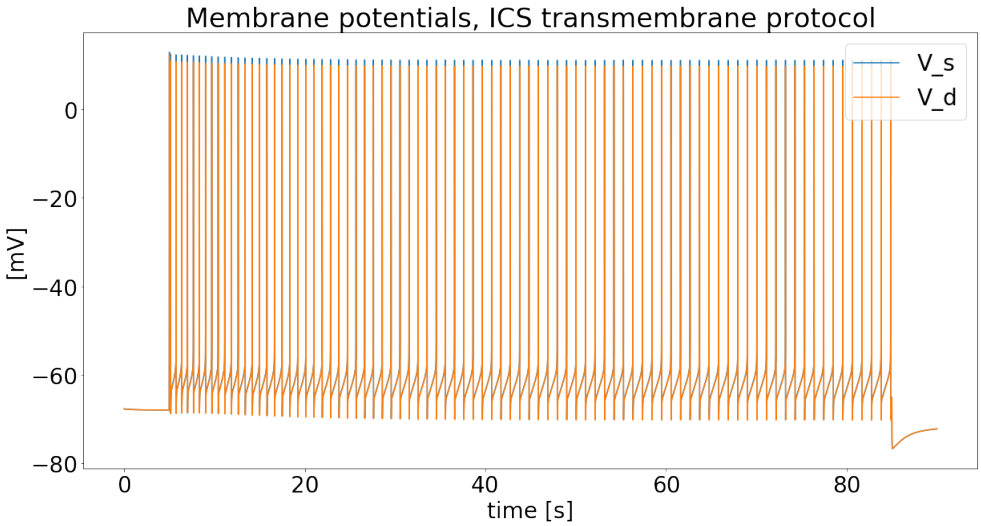

Figure 9: *Membrane potentials during the ICS protocol with injection of current into soma interior from soma exterior.*

4.3 Depolarization block

Simulations with a high stimulation current were run to study how long it will take the model to reach a depolarization block. These simulations were shorter, because depolarization block occurred within a few seconds in all protocols. For each of the 16 protocols, the neuron was stimulated with an $125pA$ current for 8 seconds. This current was sufficient to lead to a depolarization block for all protocols within the simulation time of 10 seconds. A slightly lower current, for example $110pA$, would lead to a depolarization block in some protocols and not in others. To quantify the differences in the response to this high stimulation current, the time before the depolarization block began was measured. The depolarization block was defined to begin when the neuron fired its last action potential to reach a peak over $0V$. In all cases the neuron entered the depolarization block between 1.3 and 3.2 seconds after the start of the stimulation current. The times of the start of the depolarization block is shown for all protocols in table 5.

On average, the cross-membrane stimulation took longer to lead to a depolarization block for the same current. In the transmembrane stimulation, with current across the membrane of the soma, the average time of depolarization block was 1.805 seconds after stimulation start. For the current injection into the soma from outside the system, the average time of depolarization block was 1.477 seconds after stimulation start. These averages are over all 8 ion mixes for the stimulation current.

Looking at these numbers, many of them are fairly similar for any given ion mix, whether the current is cross-membrane or external. However, there is a

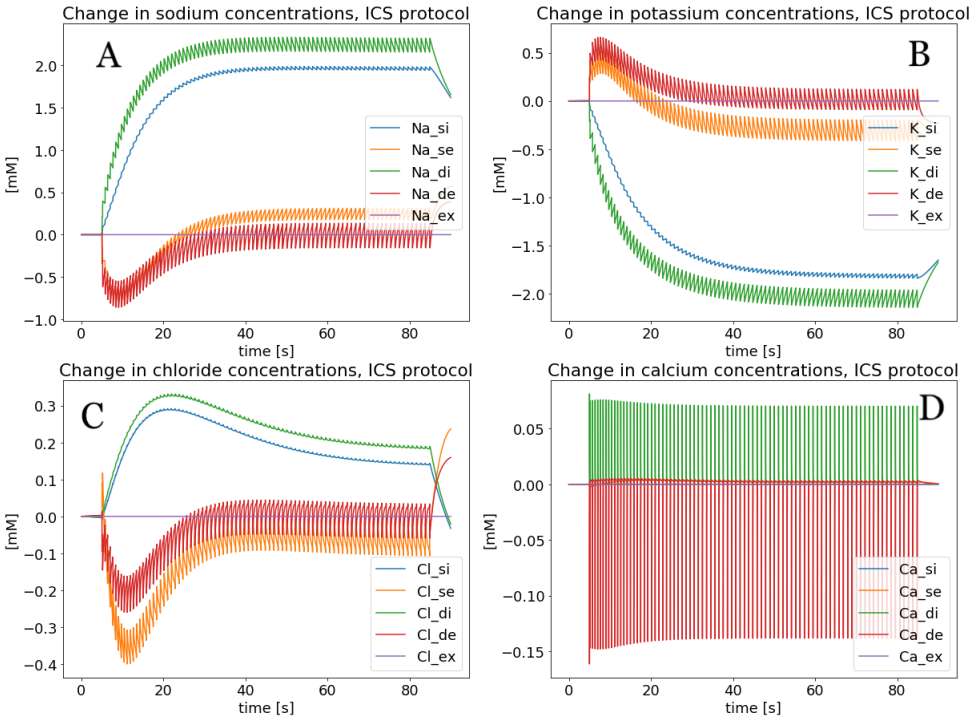

Figure 10: *Changes in concentration of ions during the ICS protocol with current into soma intercellular compartment from soma extracellular compartment. Subplots A, B, C and D show changes in* Na^+, K^+, Cl^-, *and* Ca^{2+}, *respectively.*

Protocol ion mix	Soma injection	Soma cross-membrane
ICS	1.464	2.160
ECS	1.483	1.421
$NaCl$	1.433	1.498
KCl	1.485	1.871
Na	1.602	1.515
K	1.466	3.146
Cl	1.476	1.494
X	1.404	1.331
$Average$	1.477	1.805
$Std.dev.$	0.05755	0.6067

Table 5: *Time in seconds from start of 125 pA stimulation current to last action potential before depolarization block. The bottom entry is the standard deviation of the time within the soma injection and the soma cross-membrane, respectively.*

much higher standard deviation between the cross-membrane protocols. The standard deviation for the injection currents is 0.05755 seconds, compared to 0.6067 seconds for the cross-membrane currents.

Looking at the numbers, the most striking difference is in the protocols where the stimulation current is made up of only potassium. In this case, the soma injection current leads to depolarization block in 1.466 seconds, and the soma cross-membrane current takes 3.146 seconds to do the same. This is a difference of 1.68 seconds, it takes more than twice as long for the cross-membrane current to cause a depolarization block. The next biggest differences are in the protocols with the ICS ion mix, with a difference of 0.696 seconds, and the KCl current with a difference of 0.386 seconds. In all of these cases the cross-membrane current takes longer to cause a depolarization block than the external current. All other protocols have a difference below 0.1 seconds between the time it takes to cause a depolarization block with injection current and with cross-membrane current.

What is notable about these three currents in particular, is that they all have large proportions of potassium. Looking at only the soma injection column of 5, it does not look like the currents containing potassium stand out at all, compared to the other currents. However, looking at only the columns for the cross-membrane currents, it is apparent that the currents containing potassium take longer to cause depolarization block. Not only that, but it looks like the more potassium in the current, the longer it takes to cause depolarization block. In contrast, the currents containing all or mostly sodium and chloride seem to take about the same amount of time to cause depolarization block, whether the current is from outside or across the membrane.

To summarize, when the current is coming from an external source the ion mix of the current does not greatly affect the time it takes to cause depolarization block. When the current is across the membrane, ion mixes with more potassium take longer to cause depolarization block. For currents with low or no potassium, it takes about the same amount of time to cause depolarization block whether the current is from external or internal source.

Figure 4.3 shows the membrane potentials during a strong stimulation protocol leading to a depolarization block. Note how the lowest potential reached between spikes gets progressively higher over time, which is what leads to the depolarization block.

4.4 General differences between injection and cross-membrane

Since the biggest differences seem to be between the protocols where the stimulation current contains potassium and the protocols where it does not, it seems that potassium concentrations have a strong impact on the firing rate. For the protocols where the stimulation currents were made of mostly Na^+ and/or Cl^- there was very little difference between the injection current protocols and the cross-membrane protocols.

The extracellular space has more Na^+ and Cl^- and very little K^+, while the intracellular space has more K^+, less Na^+ and even less Cl^-. This means

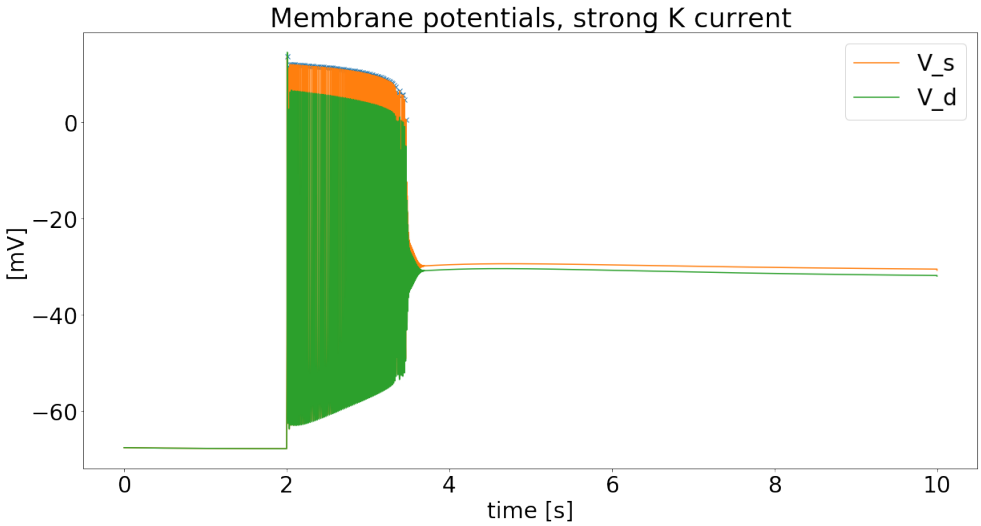

Figure 11: *Membrane potentials during high stimulation current (125 pA) with K^+ injected into soma from external source, leading to depolarization block.*

that a change in the concentration of $[K^+]$ in the extracellular compartment will be a proportionally larger than the same change in one of the other ions that may be in the stimulation current. This would lead to bigger changes in the reversal potential for $[K^+]$ and might contribute to higher firing rate.

The figures 12 and 13 plot $[K^+]_{se}$ for the injection and cross-membrane protocols, respectively. The plots are very similar for the protocols with no or low potassium. However, the protocols with potassium show a difference. In the first plot, the graphs for the protocols containing potassium are above the others. In the plot for the cross-membrane protocols this pattern is reversed.

5 Discussion and future directions

Different firing rate for different ion mixes in stimulation current

All of the protocols lead to a stable firing rate, except for the X protocol which should not be expected to be stable or realistic. There is a noticeable difference in the response of the neuron depending on which ion mix makes up the stimulation current, even though the current is the same. Notably, the stimulation currents with more potassium result in a higher firing rate with the low current, while these currents also take longer to reach a depolarization block with the high current. This means that with a stimulation current consisting of mostly potassium, the neuron can maintain a higher firing rate.

Stimulation with potassium gives a higher firing rate with the same stim-

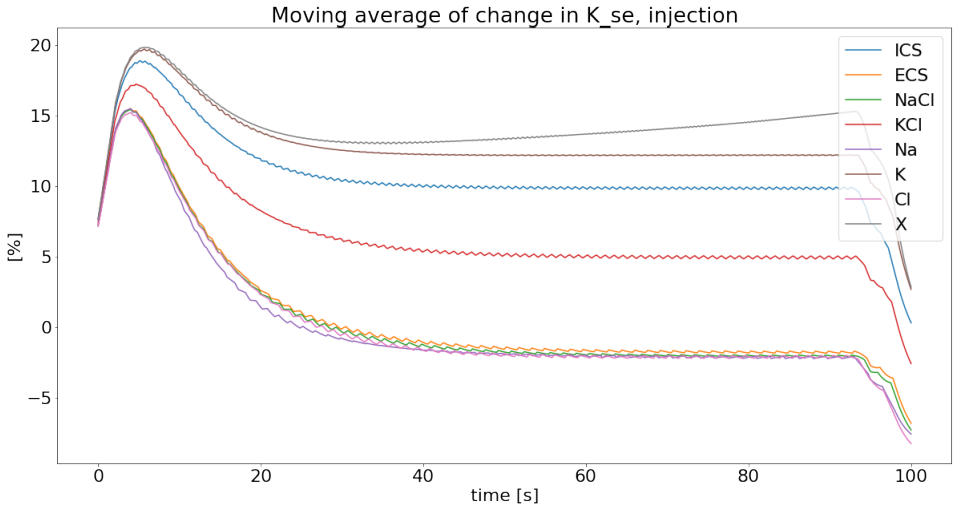

Figure 12: *Changes in concentration of K^+ in the soma extracellular compartment during all low current injection protocols. Unit of x-axis is percent change. A moving average over 50 000 time steps was used to even out the graphs enough to separate them. Otherwise the changes between each action potential would obscure the trends over time.*

ulation current, and also allows a higher stimulation current without entering depolarization block.

On average, the protocols with external injection current lead to higher firing rates, but this difference was not seen in all protocols. For the stimulation currents with ion mixes containing little or no potassium, there was little difference in the firing rate between cross-membrane and external injection currents. Likewise, there was little difference between the stimulation methods in the time before depolarization block with these ion mixes. For the protocols with stimulation currents containing potassium the firing rate was higher for injection currents than for cross-membrane currents.

Conclusions

In conclusion, the mix of ions in the stimulation currents affects the response of the model, with more potassium leading to higher firing rates at low stimulation currents as well as a tolerance for higher stimulation current. Differences between external current and cross-membrane current were more apparent in stimulation protocols containing more potassium, and minor in protocols with lower potassium.

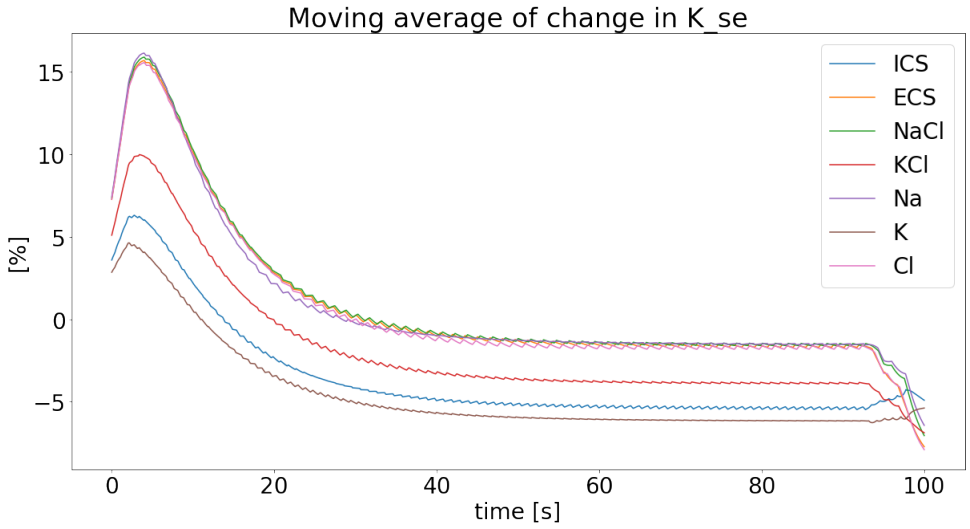

Figure 13: *Changes in concentration of K^+ in the soma extracellular compartment during all low current cross-membrane protocols except the X protocol. The latter was excluded because it the changes during this protocol were much greater than in the others, making it difficult to see differences between the other protocols. Unit of x-axis is percent change. A moving average over 50 000 time steps was used to even out the graphs enough to separate them. Otherwise the changes between each action potential would obscure the trends over time.*

Future directions - implementation of optogenetic channels

Another stimulation technique is optogenetic stimulation. This involves genetically modifying a cell so that it becomes sensitive to light[7]. Ion channels in the cell will then open when stimulated with light, which causes a current across the cell membrane which excites the neuron[7]. This means that the stimulation current in this case is made up of ions moving across the membrane from the space surrounding the cell, the extracellular space. The optogenetic ion channels can have different permeabilities to different ions, which impacts which ions actually cross the membrane when the channels open[8].

In this thesis, the "optogenetic" stimulation is simply modelled as a stimulation current where the ions move across the membrane to and from the soma external compartment. This is in contrast to the injection current simulating an electrode or pipette where the ions of the stimulation current enters the cell from outside the system. The stimulation is specified in both cases by the current that is to go into the cell. This might be a satisfactory way to specify the stimulation for the injection current, but is a naive and likely unrealistic way to specify the optogenetic stimulation. Optogenetic stimulation works by shining light on a cell, which causes ion channels in the cell to open [7]. Thus, a more realistic model would include these channels, as well as a way to specify the light

intensity on the cell instead of simply the current that is wanted. However, this would also make it more difficult to directly compare to the injection current. As the model is now, one can simply specify the same current for both cases and then compare results. With an implementation of optic stimulation the two cases would need to be compared in another way, for example by specifying a current for the injection and then finding the light intensity which will give a firing rate which corresponds to this current.

In this thesis, transmembrane stimulation is simply modelled as a current across the membrane where it is the stimulation current wanted that is specified. There is no implementation of light in the model. It would be rather straight-forward to implement both optic stimulation and optogenetic channels such as channelrhodopsin-2 (ChR2) in the model. The reason this has not been implemented here is because of the ion selectivity of the channels in ChR2. In the edPR model, only the ions Na^+. K^+. Cl^-, and Ca^{2+} are modelled, as well as the negatively charged immobile ions. However, the ChR2 channels are preferentially permeable to H^+ ions [8], which are not included in this model. In fact, the permeabilities of the ion channels are several orders of magnitude greater for H^+ than it is for any of the ions included in the edPR model[8]. Becase of this it was concluded that including ChR2 without modelling H^+ would not necessarily make the model of the optogenetic stimulation more realistic. Adding a new ion to the edPR model would be too much work to be added to this project, but is entirely possible.

Code

The code for the simulations of the five compartment edPR model used in this thesis is available at https://github.com/BirkBirkeland/EDPRmodel5compartment/

References

[1] A. L. Hodgkin and A. F. Huxley. A quantitative description of membrane current and its application to conduction and excitation in nerve. *Journal of Neuroscience Methods*, (117):pp. 500–544, 1952.

[2] D. Sterratt, B. Graham, A. Gillies, and D. Willshaw. *Principles of computational modelling in neuroscience*. Cambridge University Press, 2011.

[3] P. F. Pinsky and J. Rinzel. Intrinsic and network rhythmogenesis in a reduced traub model for ca3 neurons. *Journal of Computational Neuroscience*, 1(1):pp. 39–60, 1994.

[4] M. J. Sætra, G. T. Einevoll, and G. Halnes. An electrodiffusive, ion conserving pinsky- rinzel model with homeostatic mechanisms. *PLoS Comput Biol 16(4): e1007661*, 16(4), 2020.

[5] A. Noguchi, Y. Ikegaya, and N. Matsumoto. In vivo whole-cell patch-clamp methods: Recent technical progress and future perspectives. *Sensors*, 21(1448), 2021.

[6] K. L. Perkins. Cell-attached voltage-clamp and current-clamp recording and stimulation techniques in brain slices. *Journal of Neuroscience Methods*, 1(154):pp. 1–18, 2006.

[7] N. Grossman, K. Nikolic, C. Toumazou, and P. Degenaar. Modeling study of the light stimulation of a neuron cell with channelrhodopsin-2 mutants. *IEEE TRANSACTIONS ON BIOMEDICAL ENGINEERING*, 58(6):pp. 1742–1751, 2011.

[8] J. Y. Lin, M. Z. Lin, P. Steinbach, and Ro. Y. Tsien. Characterization of engineered channelrhodopsin variants with improved properties and kinetics. *Biophysical Journal*, 96(2):pp. 1803–1814, 2009.

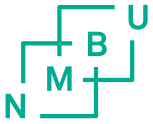

Norges miljø- og biovitenskapelige universitet
Noregs miljø- og biovitskapelege universitet
Norwegian University of Life Sciences

Postboks 5003
NO-1432 Ås
Norway